Giant Barkhausen jumps in exchange biased bulk nanocomposites sinterd fom core-shell Fe3O4-CoO nanoparticles

Thomas Gaudisson, Souad Ammar, Martino Lobue, Frederic Mazaleyrat

Giant Barkhausen jumps in exchange biased bulk nanocomposites sinterd fom core-shell Fe_3O_4-CoO nanoparticles

T. Gaudisson, S. Ammar, M. LoBue, F. Mazaleyrat, *Member, IEEE*,

***Abstract*—The magnetic behavior of spark plasma sintered Fe3O4-CoO nanoparticles is studied. The samples sintered at 500°C exhibit density over 90% and average magnetite grain size about 100 nm. When the nanocomposite is field cooled below the Néel temperature (T_N=291 K for CoO), hysteresis loops shows the expected shift with an exchange field of 80 mT at 100 K that drops down to zero approaching T_N. The coercivity at 100 K reaches 0.4 T, ten times larger than nanostructured magnetite prepared in the same conditions. When the sample is zero field cooled down to 90 K, the hysteresis loops exhibits giant Barkhausen jumps, an anomalous feature never observed before to our knowledge. The density of jumps gradually decrease on heating and disappear between 150 and 170 K. The stochastic character of the jumps is visible in the plot of the differential permeability. This new phenomenon is thought that it could be related to self-field cooling.**

***Index Terms*—exchange coupling, nanocomposites, core-shell particles**

I. Introduction

EXCHANGE bias was discovered by Bean & Meiklejohn in 1957 [1] observing that compacts made of oxidized Co fine particles cooled in a field exhibit loops shifted by a bias field H_B. This loop asymetry was explained by an exchange anisotropy between the ferromagnetic cobalt core and the anti-ferromagnetic CoO shell. The effect remained only of fundamental relevance until Peter Grunberg showed that a bottom anti-ferromagnetic layer can be used to pin the so-called reading ferromagnetic one to enhance the GMR [2]. For this kind of applications, the coercivity of the ferromagnetic layer should rather be small, so that upward and downward magnetic switching occurs at the same field ($H_C \ll H_B$) as observed by Kouvel in $(FeNi)_3Mn$ alloys [3]. However, exchange bias is not only interesting for spintronics: looking back original Bean's experiments on cobalt particles, one can observe that after field cooling, the loop is not only shifted but its coercivity almost doubled. With the constantly increasing price of rare-earth elements these last years, the idea comes that applications may not always need magnets as performing as $Fe_{14}(Nd,Dy)_2B$. As experiments show, the concept of exchange coupled soft/hard magnets (the so called spring magnets) originally proposed by Kneller [4] is not increasing the energy product of the magnets as expected [5], but can only reduced the RE content to the price of strong reduction of coercivity [6]. The problem is that, the intrinsic coercivity becomes smaller than the remanance ($H_{Ci} < M_R$), so that the material is subject to demagnetization. A first solution is to explore again well known class of materials to fill the gap between ferrite and RE magnets [7] as it was recently proposed like MnAl-C [8] and MnBi [9]. The aim of this paper is to study in which extend the exchange bias between a soft magnetic and an anti-ferromagnetic phase can yield a high coercivity material. for this purpose, we have chosen to investigate the magnetite/cobalt monoxide system witch is well adapted to core/shell particles synthesis [10].

T.G. and S.A. are with ITODYS, Universite Paris Diderot, UMR-CNRS 7086, 15 rue Jean-Antoine de Baif, F-75205 Paris, France – ammarmer@univ-paris-diderot.fr.

T.G., M.LB and F.M. are with SATIE, ENS Cachan, CNRS, 61 av du president Wilson, F-94230, Cachan, France – mazaleyrat@satie.ens-cachan.fr.

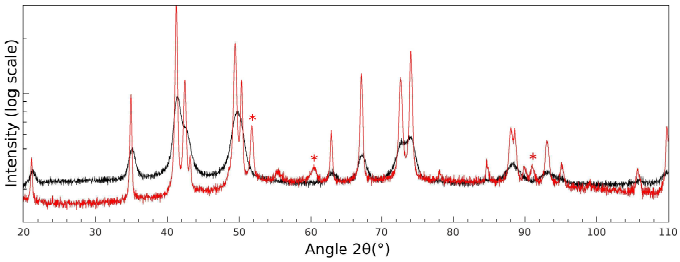

Figure 1. X-ray diffractograms of the polyol-made powder and the related SPS ceramic. The "*" symbol marks the fcc-Co phase.

II. Experimental details

A. Synthesis

a) Chemicals: Cobalt acetate and Iron acetate salts, as metal precursors, and diethyleneglycol (DEG), as solvent, were purchased from ACROS. All the reagents were used without any further purification.

b) Particles Synthesis: Iron oxide nanoparticles were prepared by forced hydrolysis in polyol medium [11]. Typically, 4 g (23mmol) of anhydrous iron acetate salt were dissolved in 250 ml of DEG and heated under reflux. Particles were recovered by centrifugation (22000 rpm), washed with acetone and dried overnignt in air. 6,23 g (25 mmol) of the recovered powder was re-dispersed in a fresh tetrahydrate cobalt acetate in DEG solution (0.1 $mol.L^{-1}$) where 0.9 mL of distilled water were added, to serve as seeds for cobalt monoxide growth. The reaction medium was then heated up to 180°C for 18 hours under mechanical stirring. The cooled suspension were centrifuged, washed with acetone, dried in air.

c) Ceramic Sintering: A Spark Plasma Sintering equipment (Syntex Dr. Sinter 515S) was used to consolidate the prepared granular composite. Typically, the powder was introduced into a 8 mm carbon die with a layer of protective papyex, without any pre-shaping. The system is closed by carbon pistons at both sides which transmit the uniaxial pressure under vacuum. DC pulses are delivered to the die by the pistons allowing the temperature to reach 500°C in three steps, in order to remove organic residue (DEG…) before sintering starts:

– heating to 280°C (at about 12 K/min) with a pressure of 50 MPa

– a plateau at 280°C increasing the uniaxial pressure from 50 to 100 MPa (at about 5 MPa/min)

– heating to 500°C (at about 30°C/min) maintaining the uniaxial pressure at 100 MPa, the soak time does not exceed 5 minutes under a load of 50 MPa.

The sintering temperature and the thermal cycle of the treatment were chosen based on the shrinkage vs. temperature curve. We assume that when the displacement of pistons slows down (volume contraction resulting from the densification) at constant pressure, the sintering process is achieved. The SPS-made pellets were polished before characterization.

d) Characterization: Powder and ceramic were characterized by X-ray diffraction (XRD) using a Panalytical XperPro equipped with a multichannel detector (X'celerator) using Co Kα radiation ($\lambda = 178.89$ pm). The cell parameter, the size of coherent diffraction domain (crystal size) and the weight ratio of each phase were determined using MAUD software, which is based on the Rietveld method combined with Fourier analysis [12]. Polycrystalline strain-free silicon was used as standard to quantify the instrumental broadening contribution.

The magnetic properties where measured using a Lake-Shore VSM model 7310 fitted with a single-stage temperature attachment operating continuously from 77 to 950 K. Susceptibility was measured continuously during cooling down to 90 K under a 10 mT field. Hysteresis loops where recorded using the following procedure: (i) heating at 450 K to ensure that cooling starts far above T_N of the AF shell, (ii) cooling down to 90 K without field (ZFC) or in a field of 1.4 T (FC), (iii) mesuring at heating by steps of 20 K under a maximum field of 1.4 T.

Table I
MAIN STRUCTURAL AND MICROSTRUCTURAL DATA INFERRED FROM MAUD REFINEMENT ON BOTH POWDER AND CERAMIC SAMPLES.

Sample	Phase	a (pm)	$\langle D_{XRD} \rangle$ (nm)	$\langle \varepsilon \rangle$	wt. %
Powder	FeO_x	840.0	17	4×10^{-3}	50
	CoO_y	427.0	9	4×10^{-3}	50
Ceramic	FeO_x	839.0	100	4×10^{-5}	56
	CoO_y	426.5	50	4×10^{-4}	37
	fcc-Co	354.0	25	2×10^{-4}	7

III. RESULTS

A. Magnetic properties of magnetite

The first point to examine is whether or not the magnetite is stoechiometric. In principle, this is very difficult to determine from XRD at room temperature. However, it is well known that magnetite undergoes a structural transition at low temperature known as Verwey transition. For stoechiometric magnetite $T_V = 119$ K and this transition is very sensitive to a lack of iron [13]. The change from cubic to orthorombic symmetry [14] results in a drastic magnetic hardening at this temperature.

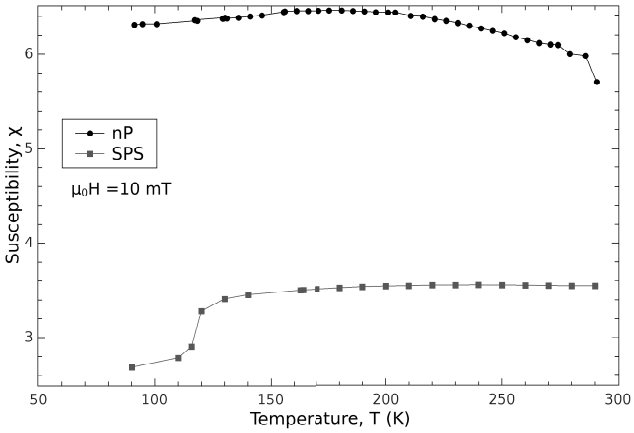

Figure 2. Susceptibility of magnetite in the form of nanoparticles (nP) and nanostructured ceramic sintered by means of SPS

In a first experiment, magnetite nanopowder directly issued from synthesis was examined. The susceptibility recorded during cooling shows a smooth maximum around 150-180 K. The hysteresis loops exhibits the typical features of superparamagnetism (zero remanance and coercivity, Langevin shaped magnetization curve) even at 90 K but the lowering of the susceptibility observed at low temperature can either be attributed to blocking or Verwey transition and doesn't enable to draw a clear conclusion on the nature of magnetite. The same powder was sintered under the conditions used for the composite. In this case, the susceptibility is sensitively smaller than that of the powder and remains nearly constant upon cooling until the drastic drop at 119 K. This figure undoubtedly due to Verwey transition which is a clear signature of the good stoechiometry of the magnetite. Hysteresis loops shows that the coercivity undergoes a dramatic drop when crossing T_V upon heating, showing again the change in magnetocrystalline anisotropy. The low coercive field observed in the SPS magnetite is compatible with its low anisotropy as observed in bulk samples and suggest that the surface anisotropy plays no significant role in the dense nanosized magnetite.

B. Exchange biased nanocomposites

In order to bring evidence of exchange bias, the composite has been field-cooled (FC) down to 90 K. The 1.4 T field was applied in the positive direction during cooling. The low temperature FC loops in Fig.4 shows the typical shift towards negative fields, but the most striking figure is the large coercivity of the exchange biased composite. Indeed, whereas the coercivity of SPS magnetite is nearly null above T_V, that of the composite is always one order of magnitude higher. Fig.5 depicts the evolution of positive (H_{C+}) and negative (H_{C-}) coercitive fields together with the exchange bias field

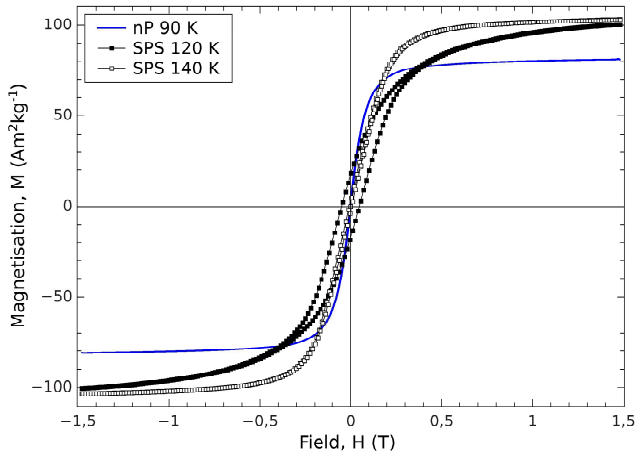

Figure 3. Hysteresis loops at low temperature of magnetite nP and SPS ceramic

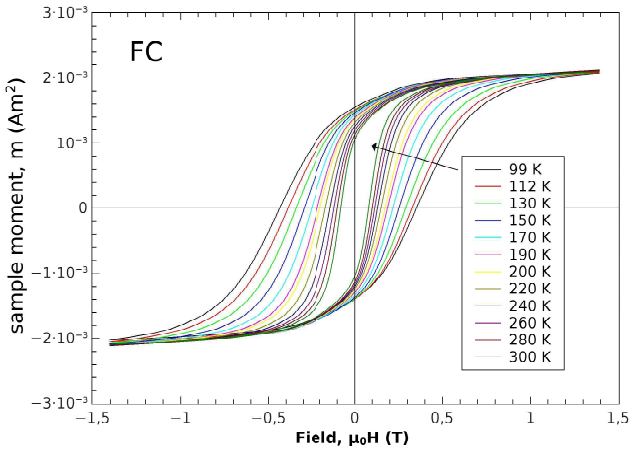

Figure 4. Hysteresis loops of field cooled nanocomposite. Saturation magnetization at 300 K is 65 $\mathrm{Am^2kgm^{-1}}$.

H_B, revealing two important figures: first, the coercivity is very close to 0,4 T, a huge value which is obtained in ferrites only with the nanostructured Ba hexaferrite [15]; second, the shift of the loop is clearly observed up to 260 K and is no more observable at 280 K, a temperature very close to the Néel point of CoO. The Considering these observations, it is clear that the exchange bias is due to ferri/anti-ferromagnetic coupling at the interface between CoO and magnetite. The $H_B = 0.1$ T found herein at 90 K, although smaller, is within the same order of magnitude as that found by Meiklejhon & Bean (up to 0.3 T). In the historic experiment, the authors measured the anisotropy constant and found a value very similar to that expected in pure cobalt. The hardening could be understood as an effect of the small grain size (about 100 nm) and the presence of the anti-ferromagnetic layer that prevent direct exchange between ferromagnetic grains, yielding coercivity closer to the anisotropy field. In other words, the AF layer helps to approach a “Stoner-Wohlfarth” behavior [16]. In the present case, even a perfect Stoner-Wohlfarth behavior would never lead such a high coercivity since $\mu_0 H_K = 2K_1/M_S \simeq 50$ mT. Thus, the hardness of the present composite can be due only to the anisotropy of the AF phase transferred to the soft one through interfacial exchange coupling.

In order to complete the analysis of FC loops, ZFC was performed and the loops measured with increasing temperature. The first loop at 99 K exhibits anomalous steps on the demagnetizing branches between remanence and opposite saturation. By increasing the temperature similar features where recorded at 112 and 130 K. The loop at 150 K still shows 2 small jumps but at 170 K the loop is absolutely similar to the FC one at the same temperature. Perusal of Fig.5 illustrate the total superimposition of H_{C+} and H_{C-} between 170 and 200 K. At low temperature, these fields differs because of the steps, which width is about 20 mT. Exchange bias field is thus determined with larger uncertainity but remains very close to that measured after FC. Looking closer the morphology of the steps, it is seen that the magnetization is nearly blocked, i.e. remains nearly constant, over a range of 15-30 mT, and then jumps. It is noticeable that this is corresponding to only 1-

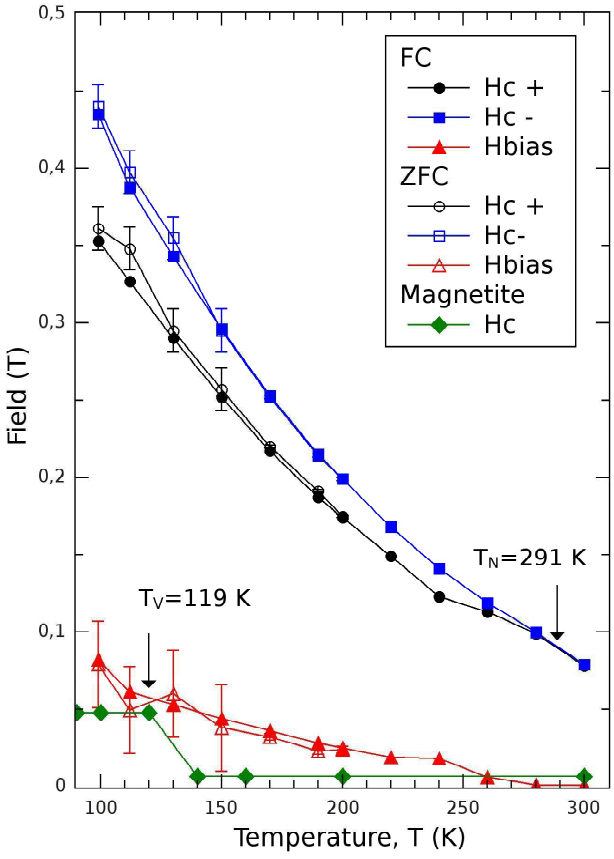

Figure 5. Coercitive (H_{C+}, H_{C-}) and bias (H_B) Fields measured on FC (full symbols) and ZFC (open symbols) nanocomposite. For comparison, H_C of SPS magnetite is also shown.

2 points of these loops (401 points/loop) and using a larger sampling fields completly hide the phenomenon. This effect is more spectacular on the differential suceptibility curves $\chi_d = \mathrm{d}M/\mathrm{d}H$. Indeed, jumps of 70 to 80% of χ_D are observed. The lower value of this figure – during blocking stage – seem to be similar to that of the demagnetizing branch but this needs deeper investigation since the sampling field step is very close to the range in which the phenomenon occurs. These

features are very similar to Barkhausen jumps appart from the fact that the latter are usually so small that they are never observed on the loop, but only by measurement of noise. In the present case, there are not more than 30 jumps in one loop and since the grain size is only 100 nm, there is no doubt that these giant Barkhausen jumps (GBJ) do not find their origin in domain wall pinning. The stochastic nature of Barkhausen noise is also found in GBJ: the same loops have been recorded several times at the same temperature both by repeating several consecutive measurements and by warming up to RT and ZFC again down to 99 K. Each time the GBJ appeared in the same region of the loop but randomly distributed. At this stage it is still difficult to explain the physical origin of GBJ, but an reasonable hypothesis could be that of a "self-field-cooling". Indeed, the magnetite particles being single domain they may form large regions coupled by dipolar interactions such as Ewing's dipolar domains observed in compas grids. The AF interface should thus experience locally fields up to magnetite saturation value $\mu_0 M_S \simeq 0.5$ T. These regions being oriented differently in space, their magnetization reversals should be distributed in field. This is consistant with the fact, appart from stochastic aspect, no field asymetry is observed in the χ_d plots (not shown here). In average, these jumps corresponds to the switch of 3% of the saturation magnetization, which for the present sample corresponds to approximately 10^{13} particles.

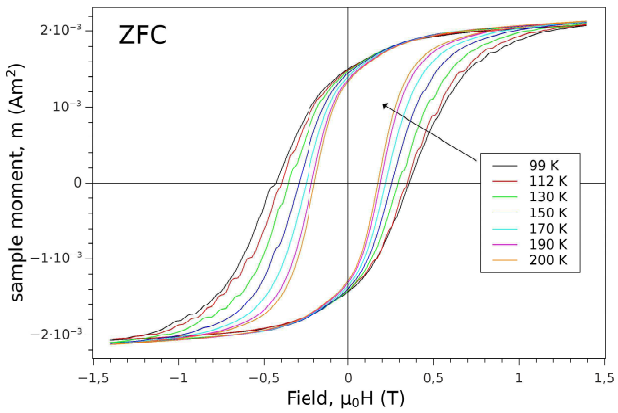

Figure 6. Hysteresis loops of zero-field-cooled (ZFC) nanocomposites. Saturation magnetization at 300 K is 65 Am^2kgm^{-1}.

In conclusion, it has been demonstrated that exchange coupled ferri/antiferro nanocomposites can be made by spark plasma sintering of core shell Fe_3O_4/CoO particles. Such composites after field cooling below the Néel temperature exhibit the expected exchange biased loops and a strong hardening with a one order of magnitude larger coercivity compared to the anisotropy field of the ferrimagnetic phase. Remarkably, this coercivity is higher than that of regular M-type hexaferrites and comparable to nanostrured ones. The most stricking figure of this nanocomposite is the giant Barkhausen jumps observed on the loops below 150 K after zero-field cooling, presumably due to self-field cooling generated by local fields in large dipolarly coupled regions.

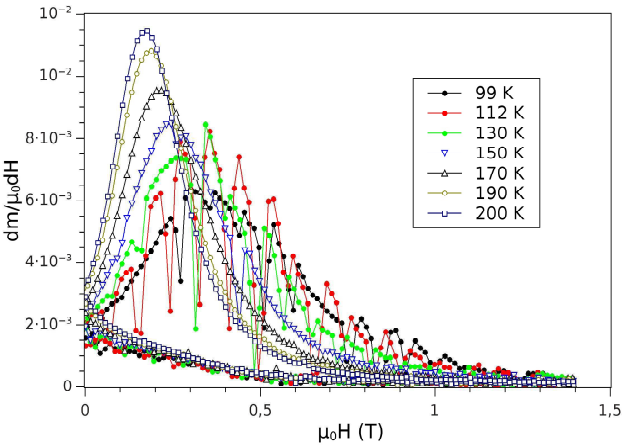

Figure 7. Differential susceptibility obtained from loops shown on Fig.X. Discontinuities are observed on the ascending branch. Only the positive field side is shown.

ACKNOWLEGMENT

This work was supported by the French National Research Agency ANR in the frame of French-Mexican project MI-NAFC

REFERENCES

[1] W. Meiklejohn and C. Bean, "New magnetic anisotropy," *Physical Review*, vol. 105, no. 3, p. 904, 1957.
[2] G. Binasch, P. Grünberg, F. Saurenbach, W. Zinn *et al.*, "Enhanced magnetoresistance in layered magnetic structures with antiferromagnetic interlayer exchange," *Physical Review B*, vol. 39, no. 7, pp. 4828–4830, 1989.
[3] J. Kouvel, C. Graham, I. Jacobs *et al.*, "Ferromagnetism and antiferromagnetism in disordered ni-mn alloys," *J. phys. radium*, vol. 20, no. 2-3, pp. 198–202, 1959.
[4] E. F. Kneller and R. Hawig, "The exchange-spring magnet: a new material principle for permanent magnets," *IEEE Trans. Magn.*, vol. 27, p. 3588, 1991.
[5] R. Skomski and J. Coey, "Giant energy product in nanostructured two-phase magnets," *Phys. Rev. B*, vol. 48, p. 15812, 1993.
[6] J. Coey, "Hard magnetic materials: A perspective," *IEEE Trans. Magn.*, vol. 47, no. 12, pp. 4671–4681, 2011.
[7] ——, "Permanent magnets: Plugging the gap," *Scripta Materialia*, vol. 67, no. 6, pp. 524 – 529, 2012.
[8] E. Fazakas, L. Varga, and F. Mazaleyrat, "Preparation of nanocrystalline mn–al–c magnets by melt spinning and subsequent heat treatments," *Journal of Alloys and Compounds*, vol. 434–435, pp. 611 – 613, 2007.
[9] K. Suzuki, X. Wu, V. Ly, T. Shoji, A. Kato, and A. Manabe, "Spin re-orientation transition and hard magnetic properties of mnbi intermetallic compound," *J. Appl. Phys.*, vol. 111, no. 7, pp. 07E303–07E303, 2012.
[10] M. Artus, S. Ammar, L. Sicard, J. Piquemal, F. Herbst, M. Vaulay, F. Fiévet, and V. Richard, "Synthesis and magnetic properties of ferrimagnetic cofe2o4 nanoparticles embedded in an antiferromagnetic nio matrix," *Chemistry of Materials*, vol. 20, no. 15, pp. 4861–4872, 2008.
[11] H. Basti, L. B. Tahar, L. Smiri, F. Herbst, M.-J. Vaulay, F. Chau, S. Ammar, and S. Benderbous, "Catechol derivatives-coated Fe3O4 and γFe2O3 nanoparticles as potential MRI contrast agents," *Journal of Colloid and Interface Science*, vol. 341, no. 2, pp. 248 – 254, 2010.
[12] L. Luterotti, "Materails analysis using diffraction," Universita di Trento, Italia, http://www.ing.unitn.it/ luttero/maud/index.html, Tech. Rep., 2003.
[13] E. Verwey and P. Haaijman, *8*, vol. 8, p. 979, 1941.
[14] S. Abrahams and B. Calhoun, "A magneto-x-ray study of magnetite at 78 degrees k," *Acta Crystallographica*, vol. 8, no. 5, pp. 257–260, 1955.
[15] F. Mazaleyrat, A. Pasko, A. Bartok, and M. LoBue, "Giant coercivity of dense nanostructured spark plasma sintered barium hexaferrite," *J. Appl. Phys.*, vol. 109, no. 7, pp. 07A708–07A708, 2011.
[16] L. Néel, "Propriétés d'un ferromagnétique cubique en grains fins," *Comptes Rendus. Acad. Sci.*, vol. 224, pp. 94–96, 1947.